ENVIRONMENTAL RESEARCH
LETTERS

LETTER • OPEN ACCESS

Estimates of ozone concentrations and attributable mortality in urban, peri-urban and rural areas worldwide in 2019

IOP Publishing Environ. Res. Lett. 17 (2022) 054023 https://doi.org/10.1088/1748-9326/ac66f3

ENVIRONMENTAL RESEARCH
LETTERS

OPEN ACCESS

RECEIVED
24 January 2022

REVISED
5 April 2022

ACCEPTED FOR PUBLICATION
13 April 2022

PUBLISHED
26 April 2022

LETTER

Estimates of ozone concentrations and attributable mortality in urban, peri-urban and rural areas worldwide in 2019

Daniel A Malashock[1], Marissa N DeLang[2], Jacob S Becker[2], Marc L Serre[2], J Jason West[2], Kai-Lan Chang[3,4], Owen R Cooper[3,4] and Susan C Anenberg[1,*]

[1] Department of Environmental and Occupational Health, Milken School of Public Health, George Washington University, Washington, DC 20052, United States of America
[2] Department of Environmental Sciences & Engineering, University of North Carolina, Chapel Hill, NC, United States of America
[3] Cooperative Institute for Research in Environmental Sciences, University of Colorado, Boulder, CO, United States of America
[4] NOAA Chemical Sciences Laboratory, Boulder, CO, United States of America
[*] Author to whom any correspondence should be addressed.

E-mail: sanenberg@gwu.edu

Keywords: ozone, air pollution, disease burden, mortality, urban, suburban, rural

Supplementary material for this article is available online

Abstract

City-level estimates of ambient ozone concentrations and associated disease burdens are sparsely available, especially for low and middle-income countries. Recently available high-resolution gridded global ozone concentration estimates allow for estimating ozone concentrations and mortality at urban scales and for urban-rural catchment areas worldwide. We applied existing fine resolution global surface ozone estimates, developed by integrating observations (8834 sites globally) with nine atmospheric chemistry models, in an epidemiologically-derived health impact function to estimate chronic respiratory disease mortality worldwide in 2019. We compared ozone season daily maximum 8 h mixing ratio concentrations and ozone-attributable mortality for urban areas worldwide (including cities and densely-populated towns), and their surrounding peri-urban, peri-rural, and rural areas. In 2019, population-weighted mean ozone among all urban-rural catchment areas was greatest in peri-urban areas (52 ppb), followed by urban areas (cities and towns; 49 ppb). Of 423 100 estimated global ozone-attributable deaths, 37% (147 100) occurred in urban areas, where 40% of the world's population resides, and 56% (254 000) occurred in peri-urban areas (<1 h from an urban area), where 47% of the world's population resides. Across 12 946 cities (excluding towns), average population-weighted mean ozone was 51 ppb (sd = 13 ppb, range = 10–78 ppb). Three quarters of the ozone-attributable deaths worldwide (77%; 112 700) occurred in cities of South and East Asia. City-level ozone-attributable mortality rates varied by a factor of 10 across world regions. Ozone levels and attributable mortality were greatest in Asian and African cities; however, cities of higher-income regions, like high-income Asia Pacific and North America, continue to experience high ozone concentrations and attributable mortality rates, despite successful national air quality measures for reducing ozone precursor emissions. The disproportionate magnitude of ozone mortality compared with population size in peri-urban areas indicates that reducing ozone precursor emissions in places that influence peri-urban concentrations can yield substantial health benefits in these areas.

1. Introduction

Tropospheric ozone is a harmful air pollutant that is associated with both short- and long-term respiratory and cardiovascular diseases [1–5]. In 2019, exposure to ozone worldwide was estimated to contribute to approximately 365 000 (95% uncertainty interval (UI): 175 000, 564 000) deaths and 6.2 (95% UI: 2.99, 9.63) million disability-adjusted life years [3]. Recent assessments have demonstrated that ozone exposure is increasing globally, driven in part by highly populated and polluted regions of Asia and Africa [6].

Furthermore, ozone air pollution is likely to continue to worsen, especially in low- and middle-income nations, driven by both emission increases and climate change [7–9]. While some regions have seen reductions in ozone and ozone precursor emissions, likely due to successful ozone management policies, harmful levels of ozone persist in some regions and are anticipated to be exacerbated by climate change [6]. While information on air pollution-related health impacts is available at national and regional levels, city-level estimates remain limited, particularly for ozone exposure and within low and middle-income countries.

Here, we leverage the recent availability of an ozone surface concentration dataset with sufficient global coverage and at relatively fine spatial resolution [6, 10] and apply a globally-consistent approach to estimate ozone-attributable mortality in cities worldwide. By using methods that are consistent across cities, we can compare how ozone-attributable mortality differs for cities that have experienced different patterns of growth and regulation. Additionally, we compare ozone levels and attributable mortality burdens across urban, suburban, and rural areas. Our approach is also compatible with the Global Burden of Disease (GBD) 2019 study, enabling consistent methods for assessing disease burdens and comparing results at varying administrative levels (i.e. regional, national, urban). Our results provide an improved understanding of the range in ozone concentrations and associated disease burden in cities worldwide, which can be used to inform air pollution and climate change mitigation actions by individual cities and across cities that are members of urban sustainability networks.

2. Methods

2.1. Health impact function

We use a commonly applied epidemiologically-derived health impact function [3, 11–13], to estimate ozone-attributable chronic respiratory disease (CRD) mortality in 2019 for urban areas worldwide (including 12 946 cities and densely-populated towns), and their surrounding peri-urban, peri-rural, and rural areas. First, we calculate population attributable fraction (PAF) at the grid-cell level (equation (1)), which represents the proportion of disease burden that would be eliminated if the risk factor were reduced to the counterfactual pollutant concentration or theoretical minimum risk exposure level (TMREL) [13]:

$$\mathrm{PAF} = \left(1 - e^{-\beta(X - X_c)}\right) \tag{1}$$

where β is the model-parameterized slope of the log-linear relationship between concentration and health endpoint from epidemiological studies, X represents the spatially and temporally resolved grid-cell level exposure estimates for ozone and X_c represents the TMREL.

We then calculate ozone-attributable mortality within each 1 km grid cell using the following equation:

$$\Delta M = \mathrm{PAF} \times \mathrm{Pop} \times y_0 \tag{2}$$

where ΔM is the disease burden (ozone-attributable deaths), Pop is the population exposed, and y_0 is the baseline mortality or disease rate within the population of interest. Subsequently, ozone-attributable deaths in each grid cell are summed according to geographical extents.

2.2. Population-weighted ozone concentrations

We calculated population-weighted ozone concentrations to incorporate spatial distributions of population in our estimation of ozone exposure (equation (3)):

$$\sum \left(\mathrm{Pop}_{k,g} \times \mathrm{Conc}_{k,g}\right) \div \sum \mathrm{Pop}_{k,g} \tag{3}$$

where Pop and Conc are the population and concentration of ozone, respectively, at the grid cell (g) within a geographical extent (k), such as the spatial boundary of a city.

2.3. Data sources

We use surface ozone estimates for 2019 which were used in the GBD 2019 study, based on DeLang *et al* [6]. They applied M3Fusion [10] and Bayesian Maximum Entropy Data Fusion [6, 14, 15] in sequence to fuse ozone ground measurement data from the Tropospheric Ozone Assessment Report [16, 17] and the Chinese National Environmental Monitoring Center Network, representing 8834 monitoring sites globally, with nine chemical transport model estimates [6]. Output was subsequently downscaled to create fine (0.1°) resolution estimates of global surface ozone concentrations (figure S1 available online at stacks.iop.org/ERL/17/054023/mmedia) by scaling relative to fine-resolution global model output, producing fine resolution estimates of ozone concentration (ppb) and variance (ppb^2) (figure S2). Estimates are available for 1990–2017 for the ozone season daily maximum 8 h mixing ratio (OSDMA8) to allow for the quantification of health outcomes from long-term ozone exposure. OSDMA8 is calculated as the annual maximum of the six-month running mean of the monthly average daily maximum 8 h mixing ratio, including through March of the following year to contain the Southern Hemisphere summer. For the GBD 2019 study, the Institute for Health Metrics and Evaluation (IHME) extrapolated the available estimates to 2019 using log-linear trends based on 2008–2017 estimates. For our analyses, we regridded ozone data for 2019 from 11 km (about 0.1°) to 1 km (about 0.0083°) resolution.

We applied a relative risk (RR) for CRD mortality of 1.06 per 10 ppb ozone (95% CI: 1.03, 1.10) derived by GBD 2019 from a meta-regression of five cohorts from Canada, the United Kingdom, and the United States [2–4, 18]. GBD 2019 applied these RR estimates for chronic obstructive pulmonary diseases (COPD) only. However, studies have shown that additional respiratory outcomes are associated with ozone exposure beyond COPD [1], and the American Cancer Society Cancer Prevention Study II, one of the largest ozone epidemiology studies used to generate the GBD RR estimates, reported RR for total respiratory disease [4]. Therefore, we apply these RR estimates with baseline disease rates for CRD mortality. For the counterfactual concentration, below which health impacts are not calculated for ozone, we used the median (32.4 ppb of ozone) of the theoretical minimum risk exposure distribution (TMRED) used by the GBD 2019 study of 29.1–35.7 ppb of ozone, based on a uniform distribution around the minimum and fifth percentile values (29.1 and 35.7 pbb, respectively) observed by Turner *et al* [4]. We used national and subnational baseline disease rates for CRD mortality for all ages from the GBD 2019 study [3]. Global population estimates for 2019 at 1 km (0.0083°) resolution were from WorldPop [19]. We evaluate the sensitivity of ozone-attributable CRD mortality estimates to the selection of key input parameters using the minimum and maximum of the TMRED, the lower and upper bound of the 95% confidence interval of the RR (1.03 and 1.10, respectively), and the 95% UI of the baseline CRD mortality rates from the GBD 2019 study. In each of these analyses, we evaluate the sensitivity of an individual input parameter, while using the central tendency estimates of the other two parameters.

To derive estimates for urban, peri-urban, and rural areas worldwide we use a modified dataset of urban-rural catchment areas (URCA) developed by Cattaneo *et al* [20] (supplementary information). Using spatial datasets from the Global Human Settlement (GHS) Layer [21, 22] and applying a least-cost-path algorithm from Weiss *et al* [23], Cattaneo *et al* [20] matched the center of urban areas to their surrounding rural populations based on the time needed to reach urban center. Each 1 km pixel is classified according to travel times (by roads, railroads, navigable rivers, and surfaces traversed by foot) to differing-sized urban areas, as either being less than 1 h (peri-urban), 1–3 h (peri-rural), or over 3 h (dispersed towns and rural hinterland).

Urban areas in the URCA dataset are comprised of boundaries for more than 13 189 cities from the GHS Grid Settlement Model (GHS-SMOD) [21] and densely populated towns from the GHS population grid model [22]. Cities are defined as having a minimum population of 0.05 million and at least 1500 inhabitants km^{-2} or a built-up area of at least 50%, and towns as having populations between 0.02 and 0.05 million. Cities are further classified into six categories according to population size, as either a large city (1–5 or >5 million), intermediate city (0.25–0.5 or 0.5–1 million), or small city (0.05–0.1 or 0.1–0.25 million). Peri-urban, peri-rural and hinterland areas in the URCA dataset define the land between urban areas. Dispersed towns are defined as isolated towns within hinterland areas of at least 5000 inhabitants. We summarize ozone-attributable CRD mortality estimates according to urban, peri-urban, peri-rural, and rural areas worldwide and by region (see supplementary data), and further stratify estimates for urban areas by cities and towns. For 243 cities, data on ozone, population, or baseline CRD mortality were not available. Consequently, our analysis includes the remaining 12 946 cities for which these data were available.

3. Results

We first evaluated population-weighted ozone and ozone-attributable mortality according to URCAs worldwide in 2019 (table 1). Population-weighted mean ozone was greatest in peri-urban areas (mean = 52 ppb), followed by urban areas (mean = 49 ppb). We estimated 423 100 deaths (95% CI of the central risk estimate: 223 200, 659 400) were attributable to ambient ozone exposure worldwide in 2019, and 157 000 (37%) of those deaths occurred in urban areas where 40% of the world's population resides. An estimated 238 000 (56%) ozone-attributable deaths happened in peri-urban areas that are within one hour of an urban center, where 47% of the world's population resides. Peri-urban areas around intermediate (0.5–1 million) and large cities (1–5 million) had the greatest number of ozone-attributable deaths (49 400 and 69 200, respectively) and the highest average population-weighted mean ozone concentrations (54 and 55 ppb, respectively) compared with any other URCA category (table S1). Large cities (>5 million) had the fourth highest ozone-attributable mortality (41 500 deaths) and fifth highest population-weighted mean ozone concentration (50 ppb) compared with all other areas. Urban areas, followed by peri-urban areas, have the highest average CRD rates (53 and 47 deaths per 100 000, respectively), as compared with other URCAs.

In nearly half of the regions worldwide, population-weighted mean ozone was greatest in peri-urban areas, compared with other URCAs (figure 1). This included regions with the largest share of global ozone-attributable deaths, South and East Asia. Regions with greater population-weighted mean ozone in urban centers included Central Latin America and High-income Asia Pacific. Andean Latin America, Central Sub-Saharan Africa, and Southeast Asia had greater population-weighted mean ozone concentrations in peri-rural areas. All areas

Table 1. Summary statistics for simple and population-weighted mean ozone season daily maximum 8 h mixing ratio concentration (ppb), average baseline chronic respiratory disease rate, ozone-attributable chronic respiratory mortality, and all-age population in 2019 according to urban-rural catchment area.

Area type[a]	Average ozone concentration (ppb)	Population-weighted mean ozone concentration (ppb)	Average baseline chronic respiratory disease rate (deaths per 100000)	Ozone-attributable chronic respiratory mortality in thousands (% of global ozone deaths)	Population in millions (% of total global population)
Hinterland (>3 h[b])	37	42	37	3 (0.8)	151 (2)
Peri-rural (2–3 h[b])	41	44	38	3 (0.8)	123 (1.6)
Peri-rural (1–2 h[b])	42	45	41	22 (5.1)	657 (8.7)
Peri-urban (0–1 h[b])	45	52	47	238 (56.3)	3586 (47.4)
Urban	48	49	53	157 (37.1)	3055 (40.3)
Towns (20k–50k[d])	48	48	51	11 (2.5)	214 (2.8)
Cities[c] (>50k[d])	48	49	53	146.4 (34.6)	2842 (37.5)
Worldwide	40	—	39	423.1 (100)	7572 (100)

[a] Statistics stratified by area type subclassifications are available in supplementary table 1.

[b] Travel time to an urban center.

[c] Cities represent 12 946 GHS-SMOD cities from Pesaresi *et al* [21].

[d] Population in thousands.

of Australasia and Oceania had population-weighted mean ozone concentrations below the TMREL.

Regionally, ozone-related deaths (figure S8) and ozone mortality rates (figure 2) were greatest in peri-urban and urban areas, followed by peri-rural areas, and hinterlands. Regional ozone-attributable mortality rates stratified by URCAs varied by an order of magnitude (range = 0.2–13.8). South and East Asia, Eastern and Western Sub-Saharan Africa, as well as most high-income regions, had greater peri-urban mortality rates compared with those of other URCAs. Regions with greater urban mortality rates included Central Latin America and Southern Sub-Saharan Africa. Southern Latin America was the only region to have its highest ozone mortality rate in hinterland areas. The remaining regions had higher ozone mortality rates in peri-rural areas or equivalent rates across either urban or peri-urban areas and peri-rural areas.

Patterns in ozone mortality rates (figure 2) within URCAs are driven largely by variation in ozone concentrations (figure 1). For example, URCAs of South and East Asia showed a similar pattern of greater ozone mortality rates and population-weighted mean ozone levels in peri-urban areas compared with other URCAs of those regions. However, inconsistencies between regions emerge, possibly reflecting the influence of other factors, such as population and baseline disease, on ozone-attributable mortality for these regions. Comparing population-weighted (figure 1) and grid-cell ozone (figure S9) concentrations, we observe influences of population distributions on ozone exposure by URCA. Additionally, patterns in ozone mortality for Central Asia and North Africa and Middle East appeared to more closely follow patterns of baseline disease rates within URCAs of these regions (figure S10). Across regions, patterns in baseline CRD rates within URCAs varied substantially. We observed higher baseline disease rates in URCAs of regions of Asia, including East Asia, as well as URCAs of some high-income regions, including North America. However patterns of baseline disease rates in most regions did not closely match patterns of ozone mortality by URCA.

Across regions, ozone-attributable mortality rates, alongside grid-cell and population-weighted mean ozone, and baseline disease rates, differed for URCAs of varying-sized cities (figures S11–S31). For example, ozone-attributable mortality rates for URCAs of East Asia (figure S18) and High-income Pacific (figure S21) were greatest for towns, small cities, and intermediate cities with inhabitants ranging from 0.02 to 0.5 million inhabitants; however, cities in these regions with populations greater than 0.5 million had higher mortality rates in peri-urban areas. These patterns in ozone-attributable mortality within URCAs, as well as the variation observed in relation to varying-sized cities, were similarly driven largely by variation in population-weighted ozone concentrations. We note that some regions may have only single values for baseline disease rates across URCAs for a particular city size because that region may only have cities of a particular size in a single country or in several with closely similar values.

To understand how ozone concentrations and attributable-mortality vary between urban areas, we evaluated estimates at the city-level (excluding towns) for 12 946 cities. In 2019, the average population-weighted mean ozone concentration across cities was 51 ppb [standard deviation (sd) = 13 ppb, range 10–78 ppb; n = 12 946]. We observed intra-region heterogeneity in population-weighted mean ozone that tended to be larger than regional average differences (figure 3; table S2). Regional

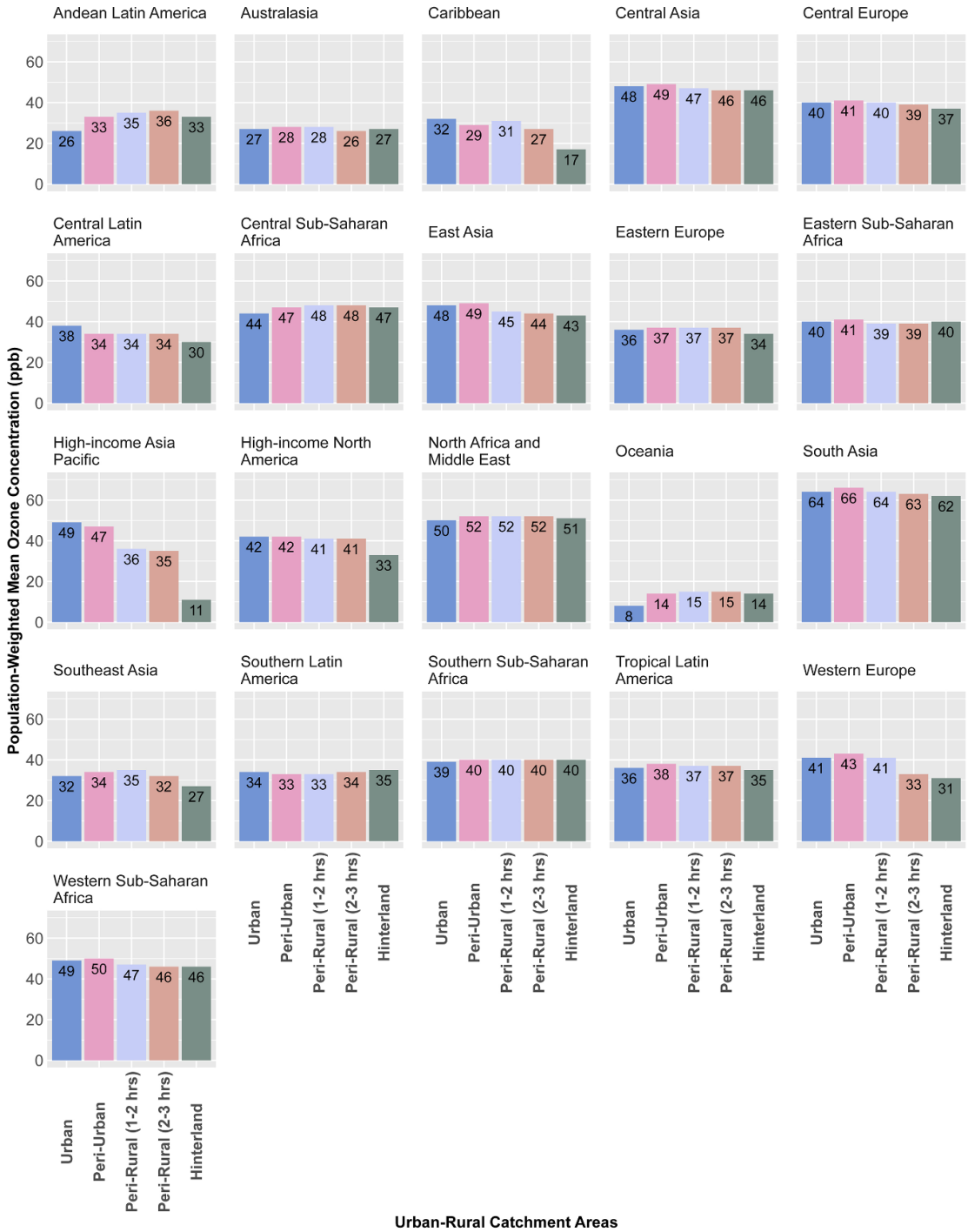

Figure 1. Population-weighted mean ozone season daily maximum 8 h mixing ratio (ppb) for each urban-rural catchment area by world region in 2019.

average population-weighted mean ozone was highest in cities of South Asia (mean = 66 ppb; n = 3939), North Africa and the Middle East (mean = 54 ppb; n = 1002), and West Sub-Saharan Africa (mean = 50 ppb; n = 909). The lowest regional average city-level population-weighted mean ozone concentrations were observed in Australasia (mean = 30 ppb; n = 31) and Oceania (16 ppb; n = 46). The remaining regions had average city-level population-weighted mean ozone concentrations between 34 ppb and 49 ppb. Of note, following cities of low and middle-income regions of Asia and Africa, those in high-income regions had the next highest population-weighted mean ozone levels. For example, cities of High-Income Asia Pacific (n = 147) and North America (n = 373), had population-weighted mean ozone concentrations of 48 ppb and 43 ppb, respectively.

We estimated that 146 400 (95% CI of the central risk estimate: 77 100, 228 700) deaths, roughly 35% of global ozone-attributable deaths, occurred in cities (n = 12 946) in 2019. For 665 (5%) cities, including

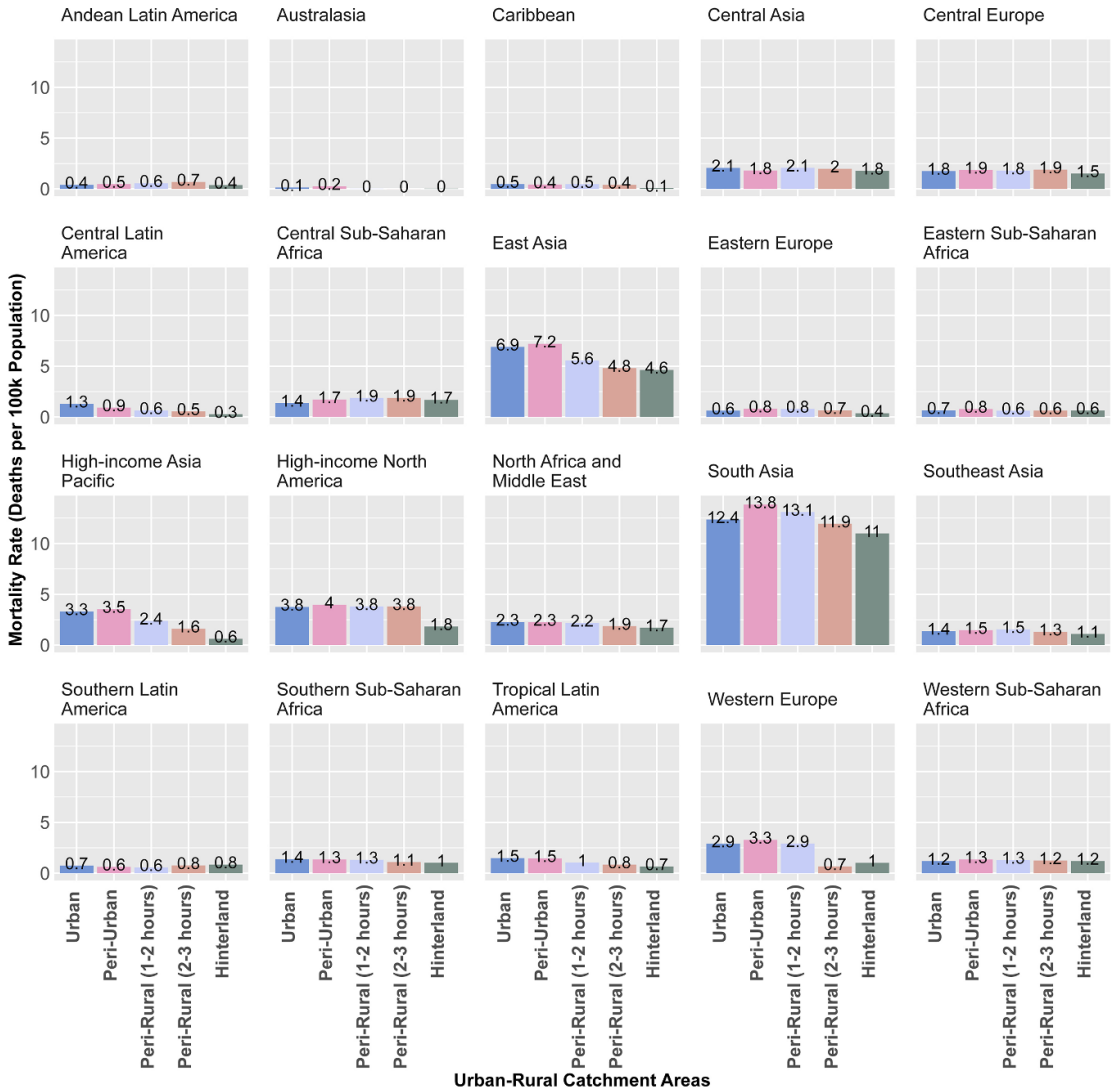

Figure 2. Ozone-attributable mortality rate for each urban-rural catchment area by world region in 2019.

all cities of Oceania, ozone concentrations were below the TMREL and ozone-attributable mortality was assumed to be zero. More than three quarters (77%; 112 700 deaths) of the ozone-attributable deaths in cities worldwide in 2019 occurred in cities of South and East Asia (47% and 29%, respectively; table S3), where 42% of the world's city-dwelling population resides. Cities located in high-income regions, including North America, Asia Pacific, and Western Europe, and North Africa and the Middle East, where 19% of the world's city-dwelling population resides, had the next highest estimated ozone-attributable mortality, with an estimated 16 700 ozone-attributable deaths (11% of the global total). Cities of India and China represented 67% of the total ozone-attributable deaths across cities (56 500 deaths [39%] and 42 000 deaths [29%], respectively; table S4). Combined, these countries have 37% of the world's population and 35% of the city-dwelling population. The countries with the next highest fraction of ozone-attributable deaths out of the total across cities were the United States, Bangladesh, and Pakistan (6800 deaths [5%], 6000 deaths [4%], 4300 deaths [3%], respectively).

The regional city-level average ozone-attributable mortality rate (deaths per 100 000 population) ranged by an order of magnitude (figure 4(a)). The highest mean mortality rates were observed in cities of South Asia (mean = 14; 69 500 deaths), followed by East Asia (mean = 7; 43 200 deaths). Cities in high-income regions, including North America, Asia Pacific, and Western Europe had the next highest estimated ozone-attributable mortality rates. Cities in Andean Latin America, Australasia, Southern Latin America, and Oceania had the lowest mean ozone-attributable mortality rates. Across cities worldwide by region, the fraction of CRD mortality attributable to ozone (%) closely resembled the distribution observed for population-weighted mean ozone concentrations by region (figure 4(b)). Mean PAF, the percent of CRD mortality, was highest in cities of South Asia (mean = 17.7%; $n = 3939$), North Africa

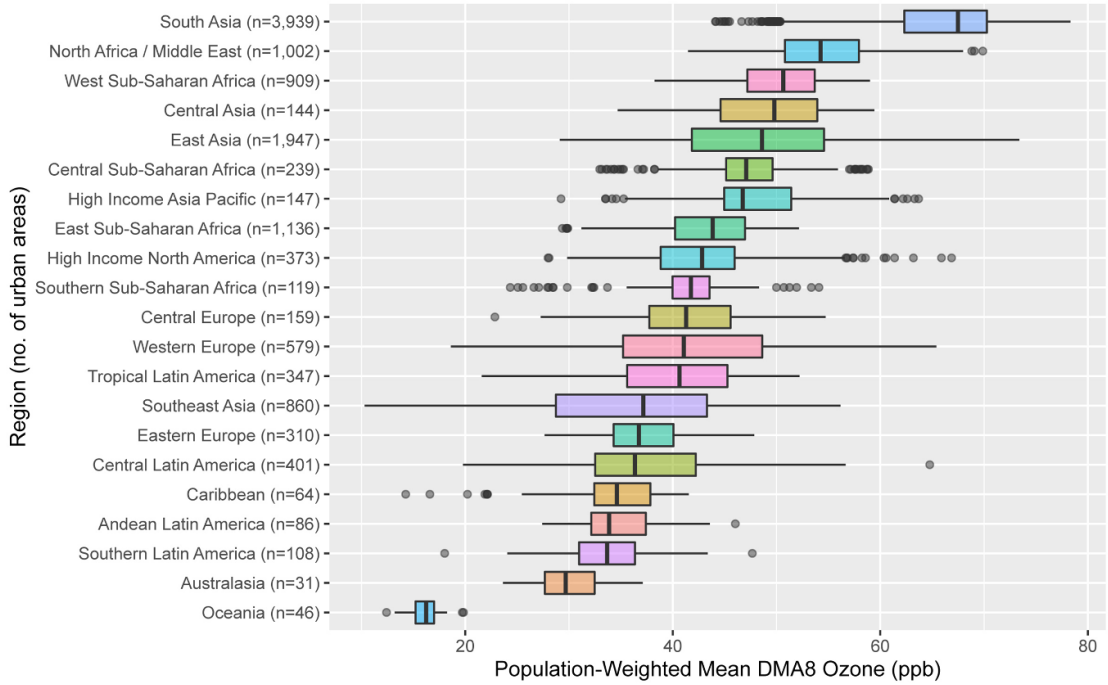

Figure 3. Population-weighted mean ozone season daily maximum 8 h mixing ratio (ppb) in 12 946 cities worldwide by region in 2019. Boxes represent the first quartile ($q_{0.25}$) to the third quartile ($q_{0.25}$) of the region-specific ozone distribution, with a bisecting line representing the median. Observations above $q_{0.75} + 1.5 \times 1QR$ or below $q_{0.25} - 1.5 \times 1QR$ were considered as potential outliers, with IQR representing the range between the $q_{0.25}$ and $q_{0.75}$.

and the Middle East (mean = 11.9%; $n = 1002$), and West Sub-Saharan Africa (mean = 9.8%; $n = 909$). The lowest regional average population-weighted mean PAFs were observed in Oceania (mean = 0%; $n = 46$), where regional ozone concentrations were below the TMREL, and Australasia (mean = 0.4%; $n = 31$). The remaining regions had mean PAFs between 1.4% and 9.3%.

Among the top 250 cities with the greatest ozone-attributable mortality, where half (51%; $n = 74\,800$) of the total ozone-attributable deaths in cities happened in 2019, deaths ranged from 75 to 3400 and population-weighted mean ozone ranged from 37 ppb to 78 ppb (figure 5). More than three quarters (77%) of the top 250 cities were in South Asia and in East Asia. Cities of India and China comprised 41% and 30% of the top 250 cities, respectively, including the top 5 cities with the greatest ozone-attributable deaths (New Delhi, India [3400 deaths; 64 ppb]; Beijing, China [2900 deaths; 66 ppb]; Kolkata, India [2700 deaths; 69 ppb]; Mumbai, India [2600 deaths; 65 ppb]; Guangzhou, China [2100 deaths; 43 ppb]).

Finally, we evaluated the sensitivity of ozone-attributable CRD mortality estimates to the selection of health impact function input parameters, including the TMREL, RR, baseline disease rate, and population estimates (figure S32 and supplementary information). We found that the selection of the RR estimate had the largest influence on estimated ozone-attributable mortality (47% decrease and 56% increase in ozone-attributable mortality, for low and high RR respectively). Compared with our analyses using ~1 km gridded population from WorldPop, we found that ozone-attributable mortality differed from our estimates by less than 3% when using ~11 km gridded global population estimates from Gridded Population of the World version 4.10, which were used in the GBD 2019 study.

4. Discussion

Our global ozone mortality estimates are similar to those reported in previous studies [3, 24]. Using similar methodology as the GBD 2019 study, we estimate roughly 15% more ozone-attributable deaths because we include all CRD (see supplementary discussion). At national and regional scales, patterns of ozone concentrations in our study are also largely consistent with those observed by other studies for ozone and fine particulate matter ($PM_{2.5}$), and similar to those for nitrogen dioxide (NO_2) with the exception of regional average exposures [3, 11, 24–26]. For example, the GBD 2019 study similarly found that annual average $PM_{2.5}$ concentrations were highest in Asia, Africa, and the Middle East. Several studies including the GBD 2019 study observed greater air pollution concentrations and mortality occurring in India and China [3, 24, 27]. Consistent with

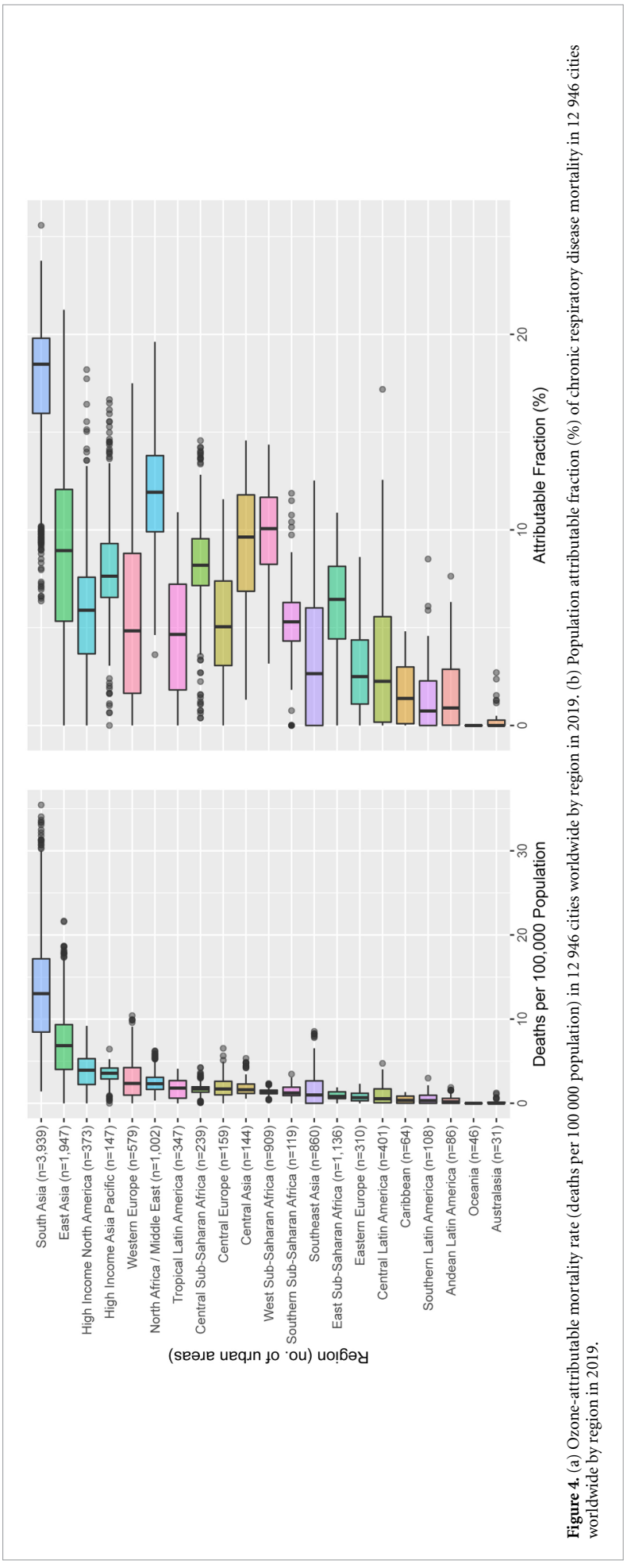

Figure 4. (a) Ozone-attributable mortality rate (deaths per 100 000 population) in 12 946 cities worldwide by region in 2019. (b) Population attributable fraction (%) of chronic respiratory disease mortality in 12 946 cities worldwide by region in 2019.

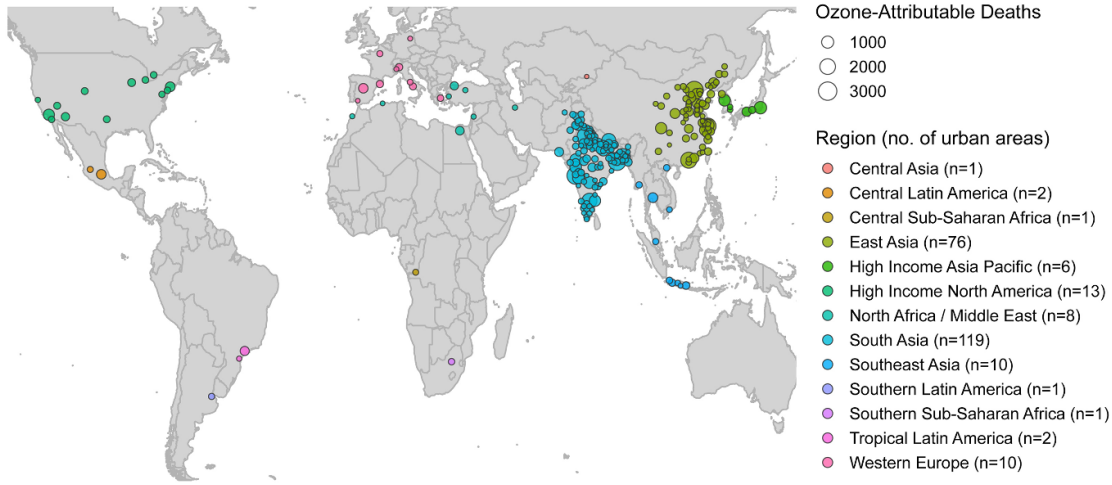

Figure 5. Number of ozone-attributable deaths for top 250 cities with the greatest ozone-attributable mortality in 2019.

our observation of high ozone burdens in high-income regions, other studies have found high NO_2-attributable pediatric asthma incidence burdens in high-income North America and high-income Asia Pacific [26, 28, 29]. While some high-income countries have experienced modest declines in ozone over the past several decades as a result of air quality improvements, air pollution burdens continue to remain high in these regions [3, 25].

Cities of Asia, Africa, and the Middle East had the highest regional average population-weighted mean ozone concentrations, compared with cities of other regions. Cities within countries of South Asia, including Nepal and India, Bangladesh, and Pakistan, had the highest or among the highest observed regional average population-weighted mean ozone concentrations. These findings are largely consistent with DeLang *et al* [6], who found that increasing trends in global population-weighted ozone over 1990–2017 were driven by highly populated and polluted regions of Asia and Africa. While ozone levels and mortality burdens were greatest in cities of low and middle-income regions of Asia and Africa, cities of higher income regions, like high-income Asia Pacific and North America, continue to experience high ozone concentrations and attributable mortality rates, despite the success of extensive air quality control for reducing ozone precursor emissions in many of these countries. Similar regional patterns for cities have been reported for concentrations of NO_2 [26, 29]. Urban populations are expected to increase worldwide, ensuring that cities, as well as the peri-urban areas that rely on them for services, will continue to be important spaces for addressing ozone exposure [30].

The fraction of ozone mortality occurring in peri-urban areas worldwide exceeded the fraction of population in those areas, which was not the case for urban and peri-rural areas. This pattern of outsized peri-urban mortality was also observed when comparing URCAs by region. Population-weighted mean ozone was greatest in peri-urban areas, followed by urban areas. Variation in ozone concentrations within regions by URCAs as well as across regions may reflect differing sensitivity regimes for ozone to nitrogen oxides (NO_x) and volatile organic compounds (VOC). Our results may in part be explained by the formation of ozone as pollution plumes move downwind of city centers, high emissions in some peri-urban areas, as well as the destruction of ozone by NO_x via NO_x titration in urban centers. In cities with more polluted urban centers, higher NO_x concentrations tend to reduce ozone concentrations in urban centers resulting in comparatively higher peri-urban ozone concentrations. Conversely, lower emissions of NO_x in some cities likely contribute to higher ozone concentrations. This finding is consistent with those of other studies [31, 32]. Additionally, Yang *et al* [33] examined ozone, NO_x, and VOC sensitivity regimes in major cities in China and found that large NO_x emissions from industry and transportation have contributed to suppressed ozone concentrations in urban areas due to the NO_x-titration effect. However, in suburban areas of some cities, the study found that the generation of ozone is less affected by anthropogenic emissions and more by the downwind migration of pollutants [33]. Further evaluation of these NO_x–O_3-VOC regimes across URCAs is needed. Additionally, while we do not expect to the see the same effect between urban and peri-urban areas for $PM_{2.5}$ and NO_x, because they have directly emitted components and are less affected by non-linear chemistry governing ozone formation and destruction, understanding of their individual contributions to air pollution risk across the urban and rural interface is also needed.

Our study and approaches have several important limitations and uncertainties. First, our analyses are limited to ozone-attributable CRD mortality based on evidence of the influence of long-term ozone exposure on mortality [4]. Consequently, our analyses do not capture acute and other short-term health effects associated with ozone exposure, such as reduced lung function, hospital admissions and emergency department visits for asthma and respiratory infections, and possible increases in asthma development [1, 34]. For example, Anenberg *et al* [11] estimated that 9–23 million annual asthma emergency room visits globally in 2015 were attributable to ozone exposure and corresponded to 8%–20% of the annual number of global visits. Additionally, ozone has been associated with non-respiratory health impacts such as cardiovascular disease, and specifically with increased rates of strokes as well as cardiac arrhythmia in persons with preexisting heart disease [1, 35, 36]. We report estimates with 95% confidence intervals on the relative risk estimate, which we identified to be the most sensitive input parameter with the widest confidence band. The relative risk estimates used in our analysis were derived from cohort studies of long-term ozone exposure in Canada, the United States, and the United Kingdom, which we apply globally for lack of alternatives, but for which there is greater uncertainty outside of these regions.

Second, there are several limitations associated with our ozone exposure data. A principal source of uncertainty in the dataset is associated with the lack of monitoring stations in large densely populated regions [6]. Specifically, spatial coverage of ozone monitoring networks is high in North America, Europe, South Korea, Japan, and China, but much lower across the rest of the world with very low data availability across Africa, the Middle East, Russia, Southeast Asia, and India. Ozone estimates in regions with fewer monitors (e.g. South Asia) are based mainly on bias-corrected model estimates and have greater uncertainty (see supplementary discussion) [6, 10]. Additionally, the ozone dataset resolves fine-scale differences in urban and peri-urban areas where there are dense monitoring networks but is less likely to resolve differences elsewhere. Third, population and baseline CRD rate estimates are uncertain, particularly for low and middle-income countries where the availability of these data is often limited. For CRD rate estimates, we relied on national and subnational CRD rates from IHME. However, subnational rates are not available for all countries, and variations at higher resolution than the subnational level likely exist. This may particularly be true when comparing urban, peri-urban, and rural populations. Lastly, as we identified in our sensitivity analyses, in addition to the selection of baseline disease rate estimates, the selection of the TMREL and RR estimates also contributes to uncertainty in our analysis.

5. Conclusion

Urban areas, including cities and densely populated towns, accounted for 40% of the global population and 37% of global ozone-attributable mortality in 2019. In contrast, peri-urban areas, where 47% of the world's population resides, accounted for 56% of global ozone-attributable mortality in 2019. Mean ozone-attributable mortality rates for cities varied by a factor of 10 across regions worldwide and appeared to be largely driven by differences in ozone exposure. We observed large inter- and intra-regional variation in city-level ozone mortality rates. While ozone concentrations and burdens were greatest in Asian and African cities, cities of higher income regions, like high-income Asia Pacific and North America, continue to experience high ozone concentrations and attributable mortality rates, despite successful air quality measures for reducing ozone precursor emissions in many of these countries. The urban and peri-urban interface has long been recognized as an important consideration for air pollution control strategies, and our findings highlight the importance of peri-urban regions for ozone-related health impacts. Our results can be used by policy makers to inform air pollution and climate change mitigation actions by individual cities and across cities that are members of urban sustainability networks.

Data availability statement

Baseline disease rates from IHME are available from http://ghdx.healthdata.org/gbd-results-tool. WorldPop datasets are available at www.worldpop.org/. Ozone datasets are available upon request from J J W (jasonwest@unc.edu). The estimated urban ozone-attributable concentrations and mortality results are available at: https://blogs.gwu.edu/sanenberg/.

All data that support the findings of this study are included within the article (and any supplementary files).

Acknowledgments

Support was provided by the NASA Health and Air Quality Applied Sciences Team (#NNX16AQ30G), the National Institute for Occupational Safety and Health (T42-OH008673), and the NOAA Cooperative Agreement with CIRES (NA17OAR4320101). Authors thank IHME for making their baseline disease rates publicly available. The views in this manuscript are those of the authors alone and do not necessarily reflect the policy of their employers. Author contributions: SCA and DAM conceptualized the project; MND, JSB, MLS, JJW, KC, and OC contributed to the development and verification of the ozone dataset used in this analysis. DAM conducted

analysis and had primary responsibility for writing the manuscript, to which all authors contributed.

Conflict of interest

The authors declare no competing interests.

ORCID iDs

Daniel A Malashock https://orcid.org/0000-0002-7454-2211
Marc L Serre https://orcid.org/0000-0003-3145-4024
Susan C Anenberg https://orcid.org/0000-0002-9668-603X

References

[1] U.S. EPA 2020 Integrated Science Assessment (ISA) for Ozone and Related Photochemical Oxidants (Final Report, Apr 2020) (Washington, DC: Environmental Protection Agency) (EPA/600/R-20/012)
[2] Jerrett M, Burnett R T, Pope C A, Ito K, Thurston G, Krewski D, Shi Y, Calle E and Thun M 2009 Long-term ozone exposure and mortality *New Engl. J. Med.* **360** 1085–95
[3] Murray C J L *et al* 2020 Global burden of 87 risk factors in 204 countries and territories, 1990–2019: a systematic analysis for the global burden of disease study 2019 *Lancet* **396** 1223–49
[4] Turner M C *et al* 2016 Long-term ozone exposure and mortality in a large prospective study *Am. J. Respir. Crit. Care Med.* **193** 1134–42
[5] WHO 2016 *Ambient Air Pollution: A Global Assessment of Exposure and Burden of Disease* World Health Organization
[6] DeLang M N *et al* 2021 Mapping yearly fine resolution global surface ozone through the bayesian maximum entropy data fusion of observations and model output for 1990–2017 *Environ. Sci. Technol.* **55** 4389–98
[7] Turnock S T *et al* 2020 Historical and future changes in air pollutants from CMIP6 models *Atmos. Chem. Phys.* **20** 14547–79
[8] Silva R A *et al* 2016 The effect of future ambient air pollution on human premature mortality to 2100 using output from the ACCMIP model ensemble *Atmos. Chem. Phys.* **16** 9847–62
[9] Fann N *et al* 2016 *Air Quality Impacts. The Impacts of Climate Change on Human Health in the United States: A Scientific Assessment* (Washington, DC: U.S. Global Change Research Program) ch 3, pp 69–98
[10] Chang K-L *et al* 2019 A new method (M3Fusion v1) for combining observations and multiple model output for an improved estimate of the global surface ozone distribution *Geosci. Model. Dev.* **12** 955–78
[11] Anenberg S C *et al* 2018 Estimates of the global burden of ambient PM2.5, ozone, and NO2 on asthma incidence and emergency room visits *Environ. Health Perspect.* **126** 107004
[12] Fann N, Lamson A D, Anenberg S C, Wesson K, Risley D and Hubbell B J 2012 Estimating the national public health burden associated with exposure to ambient PM2.5 and ozone *Risk Anal.* **32** 81–95
[13] Shaffer R M *et al* 2019 Improving and expanding estimates of the global burden of disease due to environmental health risk factors *Environ. Health Perspect.* **127** 105001
[14] Christakos G 1990 A Bayesian/maximum-entropy view to the spatial estimation problem *Math. Geol.* **22** 763–77
[15] Serre M L and Christakos G 1999 Modern geostatistics: computational BME analysis in the light of uncertain physical knowledge—the Equus Beds study *Stochastic Environ. Res. Risk Assess.* **13** 1–26
[16] Fleming Z L *et al* 2018 Tropospheric ozone assessment report: present-day ozone distribution and trends relevant to human health *Elem. Sci. Anth.* **6** 12
[17] Schultz M G *et al* 2017 Tropospheric ozone assessment report: database and metrics data of global surface ozone observations *Elem. Sci. Anth.* **5** 58
[18] Carey I M, Atkinson R W, Kent A J, van Staa T, Cook D G and Anderson H R 2013 Mortality associations with long-term exposure to outdoor air pollution in a national English cohort *Am. J. Respir. Crit. Care Med.* **187** 1226–33
[19] WorldPop 2018 The spatial distribution of population in 2019 (WorldPop) (School of Geography and Environmental Science UoSDoGaG, University of Louisville, Departement de Geographie, Universite de Namur) and Center for International Earth Science Information Network (CIESIN), Columbia University, Global High Resolution Population Denominators Project (available at: www.worldpop.org)
[20] Cattaneo A, Nelson A and McMenomy T 2021 Global mapping of urban–rural catchment areas reveals unequal access to services *Proc. Natl Acad. Sci.* **118** e2011990118
[21] Pesaresi M F, Aneta S, Marcello M and Michele M L 2019 GHS settlement grid, updated and refined REGIO model 2014 in application to GHS-BUILT R2018A and GHS-POP R2019A, multitemporal (1975–1990-2000-2015), R2019A (European Commission JRCJ)
[22] Schiavina M F and Sergio M 2019 GHS-POP R2019A—GHS population grid multitemporal (1975–1990-2000-2015) (European Commission JRCJ)
[23] Weiss D J *et al* 2018 A global map of travel time to cities to assess inequalities in accessibility in 2015 *Nature* **553** 333–6
[24] Malley C S, Henze D K, Kuylenstierna J C I, Vallack H W, Davila Y, Anenberg S C, Turner M C and Ashmore M R 2017 Updated global estimates of respiratory mortality in adults ⩾30years of age attributable to long-term ozone exposure *Environ. Health Perspect.* **125** 087021
[25] HEI 2020 State of Global Air 2020. Special Report1 (Boston, MA: Health Effects Institute)
[26] Achakulwisut P, Brauer M, Hystad P and Anenberg S C 2019 Global, national, and urban burdens of paediatric asthma incidence attributable to ambient NO_2 pollution: estimates from global datasets *Lancet Planet. Health* **3** e166–78
[27] Anenberg S C, Achakulwisut P, Brauer M, Moran D, Apte J S and Henze D K 2019 Particulate matter-attributable mortality and relationships with carbon dioxide in 250 urban areas worldwide *Sci. Rep.* **9** 11552
[28] Southerland V A, Brauer M, Mohegh A, Hammer M S, van Donkelaar A, Martin R V, Apte J S and Anenberg S C 2022 Global urban temporal trends in fine particulate matter ($PM_{2\cdot5}$) and attributable health burdens: estimates from global datasets *Lancet Planet. Health* **6** e139–46
[29] Anenberg S, Mohegh A, Goldberg D L, Brauer M, Burkart K, Hystad P, Hystad P, Larkin A, Wozniak S and Lamsal L 2021 Long-term trends in urban NO_2 concentrations and associated pediatric asthma cases: estimates from global datasets *Lancet Planet. Health* **6** e49–58
[30] UN 2018 World urbanization prospects: the 2018 revision: key facts (United Nations)
[31] Simon H, Reff A, Wells B, Xing J and Frank N 2015 Ozone trends across the United States over a period of decreasing NO_x and VOC emissions *Environ. Sci. Technol.* **49** 186–95
[32] Jhun I, Coull B A, Zanobetti A and Koutrakis P 2015 The impact of nitrogen oxides concentration decreases on ozone trends in the USA *Air Qual. Atmos. Health* **8** 283–92
[33] Yang G, Liu Y and Li X 2020 Spatiotemporal distribution of ground-level ozone in China at a city level *Sci. Rep.* **10** 7229

[34] Tian Y, Xiang X, Juan J, Song J, Cao Y, Huang C, Li M and Hu Y 2018 Short-term effect of ambient ozone on daily emergency room visits in Beijing, China *Sci. Rep.* **8** 2775
[35] Lim C C, Hayes R B, Ahn J, Shao Y, Silverman D T, Jones R R, Garcia C, Bell M L and Thurston G D 2019 Long-term exposure to ozone and cause-specific mortality risk in the United States *Am. J. Respir. Crit. Care Med.* **200** 1022–31
[36] Kazemiparkouhi F, Eum K-D, Wang B, Manjourides J and Suh H H 2020 Long-term ozone exposures and cause-specific mortality in a US medicare cohort *J. Exposure Sci. Environ. Epidemiol.* **30** 650–8